Geomechanics and Engineering, *Vol. 20, No. 2 (2020) 121-129*
DOI: https://doi.org/10.12989/gae.2020.20.2.121

Selection of design friction angle: a strain based empirical method for coarse grained soils

Emirhan Sancak[a] and Ozer Cinicioglu*

Department of Civil Engineering, Faculty of Engineering, Bogazici University, 34342, Istanbul, Turkey

(Received September 20, 2019, Revised January 3, 2020, Accepted January 4, 2020)

Abstract. In the design of geotechnical structures, engineers choose either peak or critical state friction angles. Unfortunately, this selection is based on engineer's preference for economy or safety and lacks the assessment of the expected level of deformation. To fill this gap in the design process, this study proposes a strain based empirical method. Proposed method is founded on the experimentally supported assumption that higher dilatancy angles result in more brittle soil response. Using numerous triaxial test data on ten different soils, an empirical design chart is developed that allows the estimation of shear strain at failure based on soil's peak dilatancy angle and mean grain diameter. Developed empirical chart is verified by conducting a small scale retaining wall physical model test. Finally, a design methodology is proposed that makes the selection of design friction angle in structured way possible based on the serviceability limits of the proposed structure.

Keywords: angle of dilation; friction angle; model test; particle image velocimetry; coarse grained soils

1. Introduction

Selection of the characteristic value of the friction angle in geotechnical design is an important step that influences both the economy and the safety of projects. The selection is made analyzing the results of laboratory and in-situ tests and the selected value should be representative of the considered layer. This process requires the use of correlations, theoretical considerations or empirical approaches (Bond and Harris 2008). However, when geotechnical engineers work with coarse grained soils, they have to make a more fundamental decision for the type of frictional parameter they will use in design: peak friction angle (ϕ'_p) or critical state friction angle (ϕ'_c)?

As it is very well known, mobilized value of the friction angle varies with strain and these two values can be identified with two different interpretations of the ultimate limit state. Basing design on ϕ'_c is the cautious option as it is relevant for steady state shearing conditions beyond which there is no drop in frictional characteristics for coarse grained materials. On the other hand, using ϕ'_p as the design parameter results in more economical design, however compromising safety. Unfortunately, this important decision is generally based on subjective consideration of material properties, construction processes and associated risks of failure. That is why, this study attempts to propose a more structured and mechanics based method for the selection of the type of friction angle to be used in design.

Accordingly, the first aim of this study is to develop an empirical method for predicting the necessary magnitude of shear strain that will be required for a sample of coarse grained soil to mobilize its maximum shear strength ($\varepsilon_{q\text{-}f}$). For a dense sand sample maximum shear strength corresponds to the peak of the shear stress-shear strain relationship, whereas for a loose sample it is the critical state. For this purpose, triaxial test results on ten different sand types are collected from the literature to identify and quantify the influential parameters on the magnitude of $\varepsilon_{q\text{-}f}$. Therefore, as a first step in this study, the soil properties that control the necessary amount of $\varepsilon_{q\text{-}f}$ will be identified, followed by the quantification of their influences. Resulting empirical relationships will allow the engineer to predict the magnitude of $\varepsilon_{q\text{-}f}$ for the soil. Then, in order to be able to decide whether it is possible to base design on ϕ'_p or if it is necessary to use ϕ'_c, the engineer must know the expected magnitude of the possible maximum value of shear strain that would develop in the soil if the proposed structure is allowed to deform to its serviceability limit ($\varepsilon_{q\text{-}max}$). The value of $\varepsilon_{q\text{-}max}$ is obtained using a numerical model of the proposed structure and imposing the permissible levels of deformation as prescribed displacements. The maximum value of shear strain extracted from the deformed numerical model corresponds to $\varepsilon_{q\text{-}max}$. Then design friction angle can be selected by comparing $\varepsilon_{q\text{-}f}$ with $\varepsilon_{q\text{-}max}$. Finally, in order to validate the relationship developed, a physical model test was conducted. The soil model is prepared using backfill sand that is different from the sands used in the development of the empirical relationship. As a result, a method is proposed for the selection of design friction angle based on the serviceability limits of the proposed structure.

2. Methodology

The proposed approach to the task of identifying the parameters that control $\varepsilon_{q\text{-}f}$ will require the consideration of

*Corresponding author, Associate Professor
E-mail: ozer.cinicioglu@boun.edu.tr
[a]Ph.D. Candidate
E-mail: emirhan.sancak@boun.edu.tr

ISSN: 2005-307X (Print), 2092-6219 (Online)

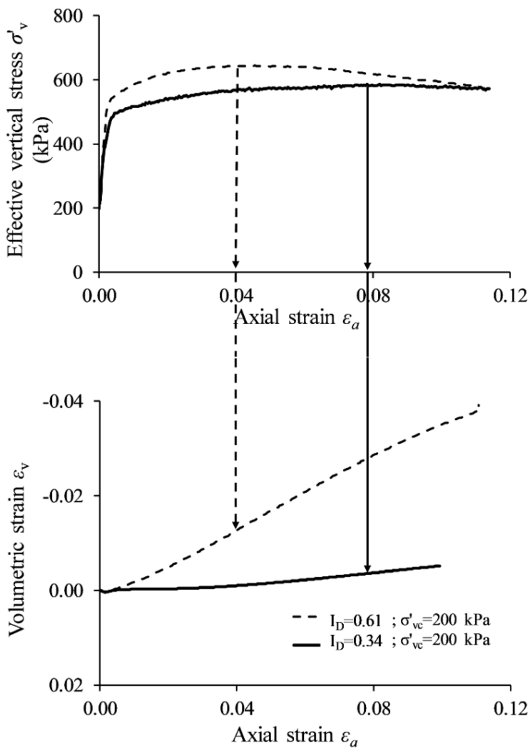

Fig. 1 Shear stress-shear strain relationships obtained from triaxial tests conducted on two Silivri sand samples

the behavior of coarse grained soils. As the goal is the estimation of $\varepsilon_{q\text{-}f}$, it is then necessary to identify and investigate different forms of responses of granular bodies to straining. It is a well-established fact that there are two general forms for the shear stress-shear strain responses of granular assemblies. In the first form, stress-strain response rises to a peak shear stress and then drops to a smaller critical state. In the second form, stress-strain response directly rises to critical state without a peak. This trend can be observed in Fig. 1 where the triaxial test results of two samples of Silivri Sand are shown. In the established custom of soil mechanics, those soils that have more pronounced peak strengths are considered denser, whereas the loosest state corresponds to the condition for which there is no peak strength and the material directly shears to ultimate state.

Many researchers since Taylor (1948) acknowledged that dilatant behavior is responsible for the above-mentioned difference between peak and critical state strengths (Lee and Seed 1967, Rowe 1969, Bolton 1986, Sasitharan 1989, Houlsby 1991, Schanz and Vermeer 1996, Cinicioglu and Abadkon 2015, Ramos *et al.* 2015, Tengattini *et al.* 2016; de Bono and McDowell 2018, Samanta *et al.* 2018). Bolton (1986) stated that the extra angle of shearing resistance measured in dense soils is correlated to its rate of dilation. The rate of dilation corresponds to the gradient of ε_a-ε_v during shear tests. As a result, rate of dilation varies throughout shearing. This is shown in Fig. 1 on the ε_a-ε_v plot for the two triaxial tests. Rate of dilation can be expressed using the familiar dilation angle form (ψ) as shown in Eq. (1) which is developed considering plane strain conditions (Bolton 1986).

$$\psi = sin^{-1}\left[\frac{-d\varepsilon_v}{d\gamma}\right] = sin^{-1}\left[\frac{-d\varepsilon_v}{d\varepsilon_1 - d\varepsilon_3}\right] \tag{1}$$

Here, $d\varepsilon_v$ is volumetric strain, $d\gamma$ is shear strain, $d\varepsilon_1$ and $d\varepsilon_3$ are major and minor principal strains in incremental forms. Schanz and Vermeer (1996) extended the formulation to consider axisymmetric conditions based on the stress-dilatancy theory proposed by Rowe (1962). This study uses the equation proposed by Schanz and Vermeer to calculate the magnitude of ψ from the results of triaxial tests, which is given as Eq. (2).

$$\sin\psi = -\frac{d\varepsilon_v/d\varepsilon_1}{2 - d\varepsilon_v/d\varepsilon_1} \tag{2}$$

Owing to the incremental forms of Eqs. (1)-(2), rate of dilation varies throughout shearing. The maximum of the rate of dilation corresponds to the peak angle of dilation, ψ_p. Peak shear strength and ψ_p mobilize simultaneously in accordance with the well-known observation in literature (Bolton 1986, Vaid and Sasitharan 1992, Chakraborty and Salgado 2010). This is an outcome of the fact that peak strength for soils is an outcome of the work done to overcome interlocking. The same trend can be observed also in Fig. 1 as for all the tests used in this study. Shear resistance in excess of critical state strength is then associated with ψ_p.

The magnitude of ψ_p is dependent on the combined influences of soil density and stress state (Rowe 1969; Bolton 1986; Cinicioglu and Abadkon 2015). These are the same variables which also control the form of the stress-strain relationships for soils. Hence, ψ_p is a deformation parameter that directly influences strength. Furthermore, Soltanbeigi *et al.* (2019) noticed that greater ψ_p of granular assemblies results in thinner shear bands at failure and these yield more brittle responses. This property of ψ_p then suggests a possible relationship that requires investigation between ψ_p and $\varepsilon_{q\text{-}f}$. However, there is no study in literature that investigates the required magnitude of strain to mobilize ψ_p and therefore to reach peak failure. Accordingly, the goal of this study is to experimentally investigate and to empirically quantify the relationship between $\varepsilon_{q\text{-}f}$ and ψ_p.

Fig. 1 visually illustrates the anticipated trend of the $\varepsilon_{q\text{-}f}$ -ψ_p relationship. In Fig. 1, both samples are consolidated under the same vertical effective stress (σ'_{vc}). Therefore, the test with the higher relative density (I_D) yields the greater ψ_p. As expected, higher ψ_p results in earlier peak failure. This response is embedded even in constitutive models of soils. For example, in case of hardening soil models of dense sands or heavily overconsolidated clays, shear stress-shear strain response is dominantly elastic until the peak response is reached. That results in stiffer response that reaches peak strength with relatively less straining compared to the responses of loose sands or normally consolidated clays (Muir Wood 1990). This means that the magnitude of $\varepsilon_{q\text{-}f}$ is smaller for soils with greater ψ_p magnitudes. For loose granular soils, the necessary magnitude of $\varepsilon_{q\text{-}f}$ is greater and majority of strength tests

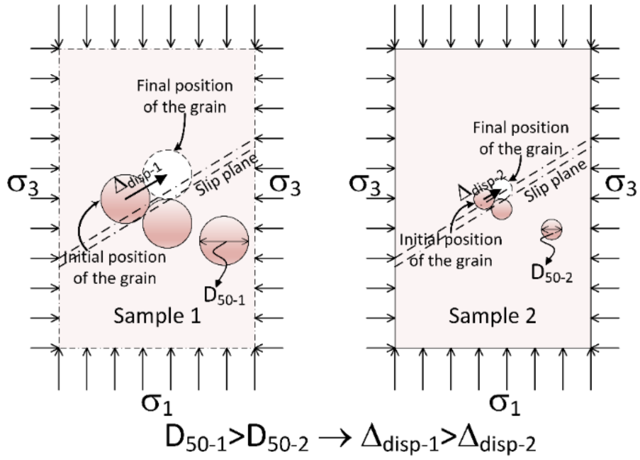

Fig. 2 Necessary magnitude of displacement to overcome interlocking (Δ_{disp}) is dependent on the average sizes of soil grains (D_{50}). The relative size of the displacement vector with respect to sample size is an indicator of expected strains

Table 1 Main properties of sands used to develop the relationships

Sample	G_s -	e_{max} -	e_{min} -	D_{50} mm	C_c -	C_u -	Reference
Silivri Sand	2.67	0.96	0.56	0.37	1.45	2.16	(Cinicioglu and Abadkon 2015)
Erksak Sand	2.66	0.78	0.53	0.34	1.00	1.90	(Sasitharan 1989)
Salt Lake Sand (Sereflikochisar)	2.62	0.86	0.50	1.13	1.12	2.24	(Erzin 2004)
Bafra Sand	2.68	0.61	0.41	0.60	0.83	3.48	(Erzin 2004)
Sinop Sand	2.64	0.80	0.58	0.31	1.12	1.24	(Erzin 2004)
Ceyhan Sand	2.70	0.82	0.54	0.30	1.13	2.19	(Erzin 2004)
Ankara	2.64	0.65	0.40	0.90	1.50	5.80	(Erzin 2004)
Yumurtalik	2.70	0.81	0.56	0.22	1.08	1.76	(Erzin 2004)
Sile	2.61	0.78	0.52	0.71	1.12	2.8	(Arda 2019)
Kilyos	2.66	0.77	0.44	0.26	0.97	1.24	(Arda 2019)

conducted for practical purposes are triaxial compression tests. The authors acknowledge that $\varepsilon_{q\text{-}f}$-ψ_p relationships might vary for different stress paths, but no single stress path is relevant for the entire lengths of shear bands that develop in soils supporting full-scale structures. When deformation zones underneath foundations are considered, different sections of shear bands might correspond to different modes of shearing (i.e., compression, extensional) (Houlsby 1991, Bardet 1997). For example, when the bearing capacity failure of a shallow foundation is considered, the form of the stress path experienced by soil depends on the position along the length of the resulting failure planes. Within the active wedge, triaxial compression type of loading is more appropriate, whereas within the passive wedge, the stress path is more similar to triaxial extension. Therefore, defining the relationships considering triaxial compression test results is a practice oriented choice, since these are more routinely conducted.

For the evaluation of the proposed design chart, a small scale physical 1g model retaining wall test was conducted

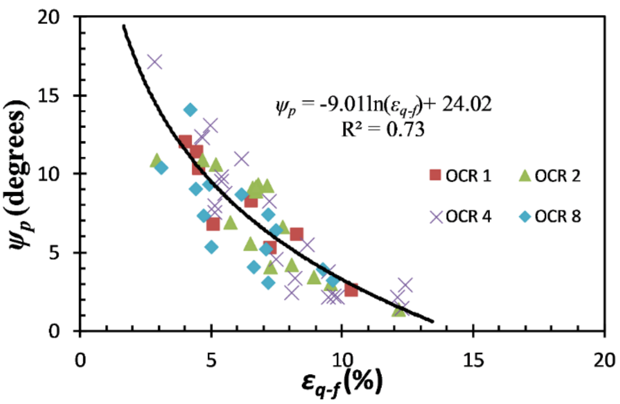

Fig. 3 Comparison of ψ_p - $\varepsilon_{q\text{-}f}$ relationships of different OCR samples of Silivri Sand and the collective exponential best-fit line

using a different sand than the ones used in the development of the chart. Examining the images captured during the model test with an image-based deformation method called Particle Image Velocimetry (PIV) (White *et al.* 2003), the actual values of $\varepsilon_{q\text{-}f}$ are obtained. The predicted value of $\varepsilon_{q\text{-}f}$ and the actual values of $\varepsilon_{q\text{-}f}$ measured using PIV are compared to each other and the results are discussed. Finally, a method for the selection of the appropriate design friction angle is proposed.

3. Material properties

This study comprises two parts. The first part involves the investigation of different sands for defining the relationship between $\varepsilon_{q\text{-}f}$ and ψ_p. In the second part, defined empirical relationship is evaluated by conducting a physical model test. The data collected for the first part of the study comes from triaxial compression tests conducted on ten different sands. This dataset of ten sands excludes the sand used in the model test conducted for verification (Akpinar Sand). The complete dataset used for the development of the proposed design chart is provided in an open data repository as a supplementary material (Cinicioglu and Sancak 2019). The material properties of these sands are summarized in Table 1. As it can be observed there, gradation characteristics of these sands are significantly different from each other. However, the results of triaxial tests conducted with Akpinar sand are not used in the development of the proposed design chart: its material properties are given in the section titled “The model test”.

4. Obtained results

Obtained datasets of each of ten sands are used to plot the variations of $\varepsilon_{q\text{-}f}$ with ψ_p. One of the sands investigated is Silivri Sand. Triaxial tests on this sand were conducted in the laboratory of the Bogazici University for the investigation of dilatant behavior (Abadkon 2012). Reconstituted samples prepared with Silivri Sand were prepared and tested at different combinations of relative

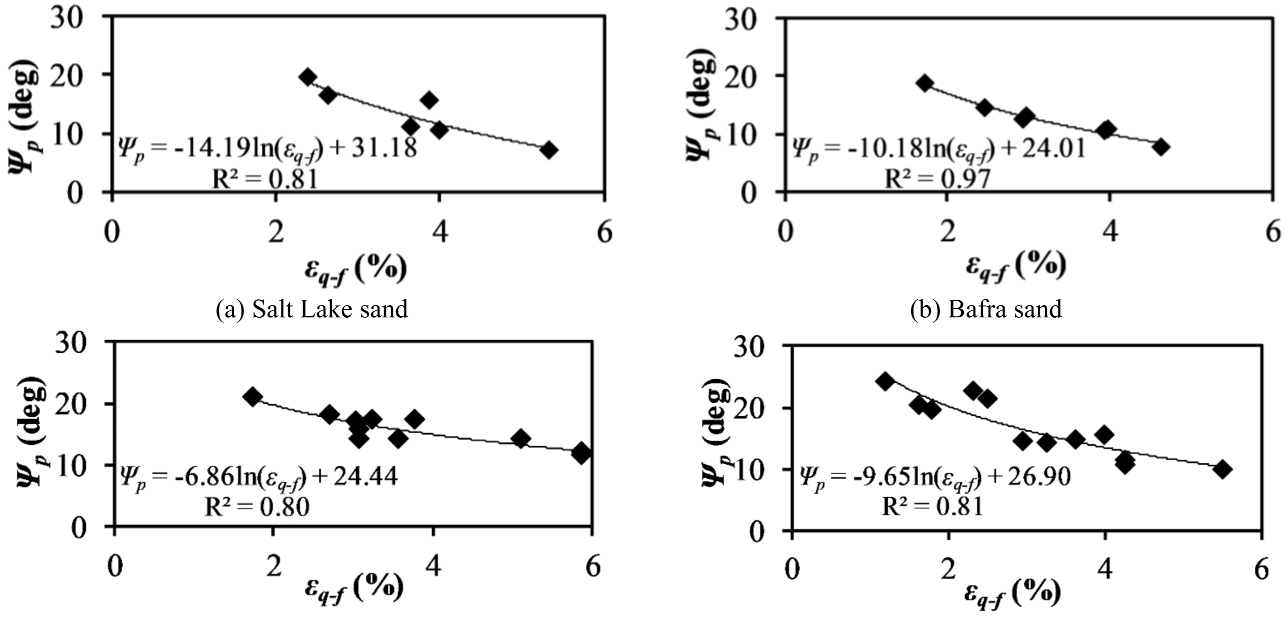

(a) Salt Lake sand (b) Bafra sand

(c) Sinop sand (d) Ceyhan sand

Fig. 4 Examples of ψ_p - $\varepsilon_{q\text{-}f}$ relationships

Table 2 Fitting parameters of empirical equations for each sand

Sand	α	β
Erksak	8.49	21.67
Silivri	9.01	24.02
Bafra	10.18	24.01
Sinop	6.86	24.44
Salt Lake (Sereflikochisar)	14.19	31.18
Ceyhan	9.65	26.90
Ankara	11.39	29.84
Yumurtalik	8.71	25.12
Sile	14.60	24.90
Kilyos	7.38	21.60

density and mean effective stress. Additionally, these samples tested at different combinations of relative density and mean effective stress were prepared at four different overconsolidation ratios (OCR). The availability of data at different OCRs presents the possibility of checking whether stress history has an influence on the probable relationship between $\varepsilon_{q\text{-}f}$ and ψ_p. For this purpose, the triaxial test results of Silivri Sand at four different OCRs are used for plotting Fig. 3. Evident in Fig. 3, the relationship between $\varepsilon_{q\text{-}f}$ and ψ_p is not influenced by OCR. This observation is important within the context of this paper as it is necessary to show that $\varepsilon_{q\text{-}f}$ - ψ_p relationship is not affected by the stress history of the soil. Since $\varepsilon_{q\text{-}f}$ - ψ_p relationships are not affected by stress history, then the magnitude of $\varepsilon_{q\text{-}f}$ will be directly dependent on ψ_p for a single soil (Sancak 2014). This is an expected outcome because ψ_p also includes the effects of loading and unloading behavior as greater OCR corresponds to more densely packed granular configurations for the considered confining pressures.

Fig. 3 additionally shows that $\varepsilon_{q\text{-}f}$ - ψ_p relationships can be approximated using a logarithmic function. When $\varepsilon_{q\text{-}f}$ - ψ_p relationships for different sands are investigated, it is noticed that their general forms are similar (Fig. 4) and the same logarithmic function can be used for all sands independent of their OCR values.

Accordingly, for practical purposes it is decided that the relationship between $\varepsilon_{q\text{-}f}$ and ψ_p can be simulated by a logarithmic function as given in Eq. (3).

$$\psi_p = -\alpha \ln \varepsilon_{q-f} + \beta \tag{3}$$

where α and β are empirical line-fitting parameters. This equation is a unit-dependent empirical equation and the input value, $\varepsilon_{q\text{-}f}$, is inserted as percentage whereas the output, ψ_p, is in degrees. The values of the empirical line-fitting parameters α and β vary with sand type as shown in Fig. 4. The values of all line fitting parameters for all investigated soils are collected in Table 2.

As explained in the methodology section, the variations of the line-fitting parameters of Eq. (3) must be investigated by taking the discrete particulate nature of granular skeletons into account. Hence, variations of the empirical line-fitting parameters with D_{50} are investigated for all the sands of this study except the sand used as physical model backfill. Obtained relationships of α-D_{50} and β-D_{50} are shown in Fig. 5 where they are approximated by simple linear regression.

Resulting empirical relationships are shown in Eqs. (4)-(5):

$$\alpha = 7.17D_{50} + 6.36 \tag{4}$$

$$\beta = 7.90D_{50} + 21.31 \tag{5}$$

These equations are unit-dependent and the appropriate

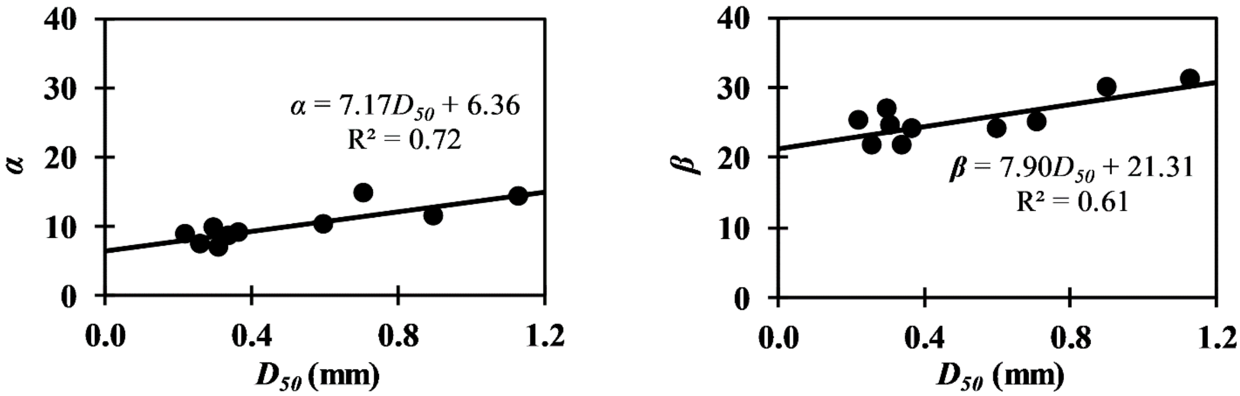

(a) α - D_{50} relationship (b) β - D_{50} relationship

Fig. 5 The relationship between fitting parameters, α and β, and average grain size, D_{50}

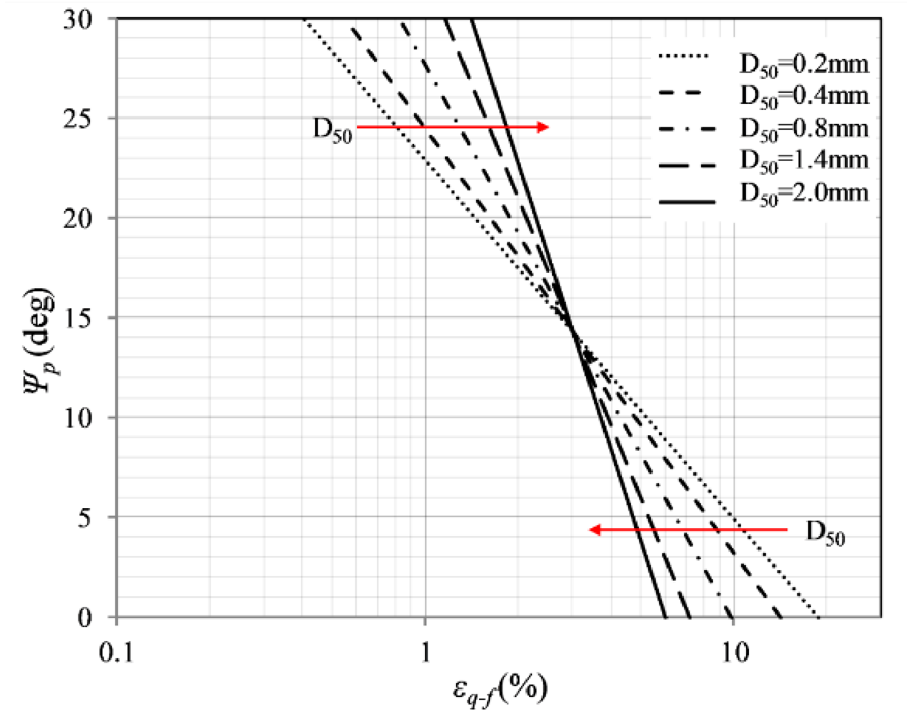

Fig. 6 Design chart that allows the estimation of $\varepsilon_{q\text{-}f}$ based on the D_{50} of sand and the ψ_p.

Table 3 Engineering properties of Akpinar sand

Sand Type	e_{max}	e_{min}	D_{50}	C_u	r	ϕ'_{cv}	I_D
Akpinar	0.87	0.52	0.27 mm	1.23	0.39	33.8^0	0.8

unit for D_{50} in these equations is mm. Hence, Eqs. (4)-(5) were combined with Eq. (3) and rearranged to yield $\varepsilon_{q\text{-}f}$ in terms of ψ_p and D_{50}, as shown in Eq. (6):

$$\varepsilon_{q-f} = e^{\frac{\psi_p - 7.90D_{50} - 21.31}{-7.17D_{50} - 6.36}} \tag{6}$$

Empirically obtained Eq. (6) is used to develop a design chart as shown in Fig. 6. Dashed linear lines represent the variations of $\varepsilon_{q\text{-}f}$ with ψ_p for given D_{50} values. For a sand that has a D_{50} value that does not fall on a line already drawn in Fig. 6, a new line can be drawn using Eq. (6).

5. The model test

A physical model test is conducted to evaluate the design chart given in Fig. 6. The model setup, which is illustrated in Fig. 7, simulates active failure by lateral wall translation. The sides of the model box are plexiglas to allow the monitoring of deformation in the backfill. This allows photographing different stages of the test for later analyzing using PIV (Stanier *et al.* 2016). PIV is a digital image-based displacement measurement method that tracks particle flow. PIV achieves this by examining images captured at different instances of deformation using the initial image corresponding to no deformation state as a

(a) Photograph of the setup with the pluviation and data acquisition systems

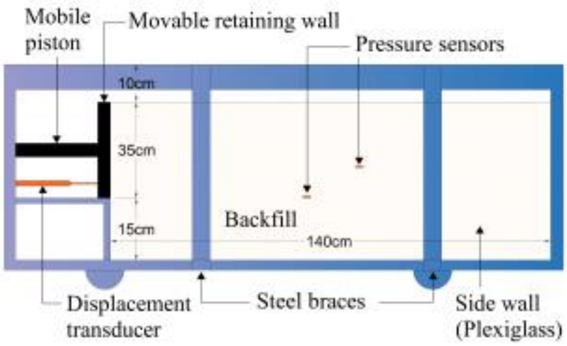

(b) Cross-section of the physical model setup

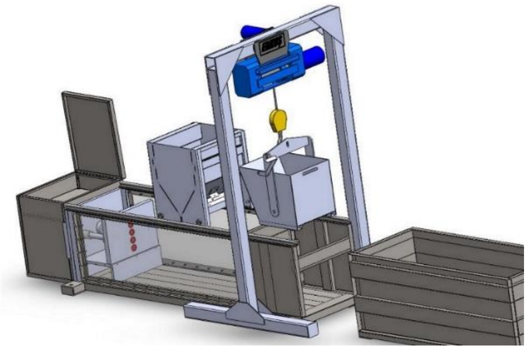

(c) Illustration of the system

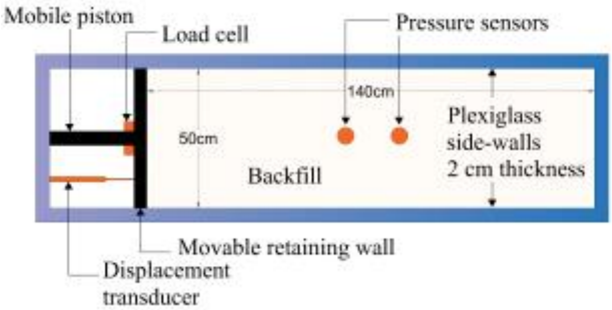

(d) Plan view of the physical model setup

Fig. 7 Physical model setup

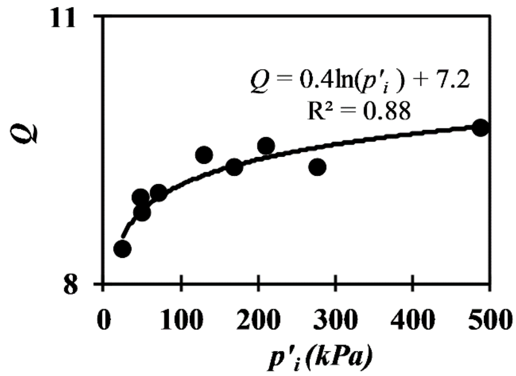

(a) Q versus lnp'_i relationship

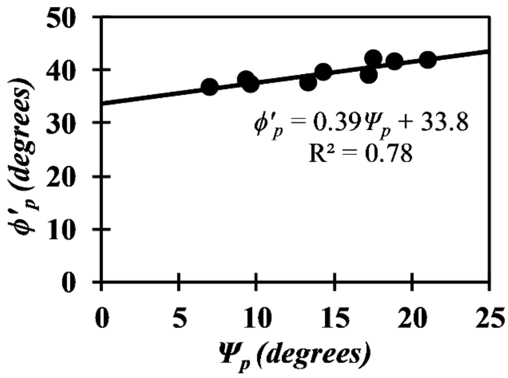

(b) ψ_p versus ϕ'_p relationship

Fig. 8 Relationships for obtaining the necessary line-fitting parameters for Akpinar Sand

reference. Detailed information on PIV can be found in Gezgin and Cinicioglu (2019), Altunbas *et al.* (2017), White *et al.* (2003), and Stanier *et al.* (2016). In this study, a Matlab based PIV software called GeoPIV (White *et al.* 2003), specifically developed for geotechnical problems, is used. Model backfill is prepared using dry-pluviation (Kazemi and Bolouri 2018). The pluviation height is kept constant to achieve a homogeneous backfill. Properties of Akpinar sand used as a backfill throughout the model tests are shown in Table 3. Five density cans are placed in the backfill in positions that will not interfere with the developed shear bands. The density cans are exhumed after the test is completed to measure the backfill soil's unit weight.

Five soil pressure transducers are located on the face of the model retaining wall. Moreover, two miniature soil pressure transducers are placed within the backfill. These miniature pressure transducers are used to measure the magnitudes of vertical and horizontal stresses in the soil.

The test is conducted by translating the model wall away from the backfill soil at constant rate. Photographs are captured using a high rate camera at various stages of the test.

In order to be able to use the design chart (Fig. 6), the magnitude of ψ_p needs to be calculated. This is achieved using the empirical equation proposed by Bolton (1986):

$$\psi_p = \frac{A_\psi}{r} I_R = \frac{A_\psi}{r}\left[I_D\left(Q - \ln\frac{100p'_f}{p_a}\right) - R\right] \quad (7)$$

where p'_f is the mean effective stress at failure, I_D is relative density, and p_a is the atmospheric pressure. The values A_ψ are 3 and 5 for axisymmetric and plane strain conditions, respectively (Bolton 1986). Q, R and r are line-fitting parameters that are obtained by triaxial testing. The parameter I_R is called the relative density index and considers the influence of confinement on relative density (Bolton 1986). For both plane strain and axisymmetric conditions, Bolton (1986) showed that the magnitude of I_R is directly dependent on the maximum gradient of the ε_1-ε_v relationship (Eq. 8).

$$\left(-\frac{d\varepsilon_v}{d\varepsilon_1}\right)_{max} = 0.3I_R \tag{8}$$

Then, using Eq. (8), the value of I_R can be calculated based on the results of the experiments. Following the suggestion of Bolton (1986), the value of the line-fitting parameter R is selected as 1. Rearranging Eq. (7) for I_R, the magnitude of the line-fitting parameter Q can be obtained using Eq. (9).

$$Q = \frac{I_R + R}{I_D} + \ln p'_f \tag{9}$$

According to Chakraborty and Salgado (2010), especially for small confining pressures, the value of Q is dependent on the initial value of mean effective stress (p'_i) as given in Eq. (10).

$$Q = \zeta \ln p'_i + \eta \tag{10}$$

The values of the line-fitting parameters ζ and η suitable for Akpinar Sand are obtained from the results of triaxial tests by plotting best-fit Q values against p'_i as shown in Fig. 8a. Their values are 0.4 and 7.2, respectively.

On the other hand, the line-fitting parameter r is defined by Bolton (1986) following the observation of Bishop (1971) that the relationship between ϕ'_p and ψ_p is linear. Based on this observation, the line-fitting parameter r is calculated as the slope of this relationship where the zero-intercept is ϕ'_c. Resulting relationship is given as Eq. (11) and the ψ_p-ϕ'_p relationship of Akpinar Sand is shown in Fig. 8(b). Based on the data given in Fig. 8(b), the values of r and ϕ'_c are 0.39 and 33.8^0, respectively.

$$\phi'_p = \phi'_c + r\psi_p \tag{11}$$

Then, all the obtained line-fitting (R, ζ, η, r, ϕ'_c) parameters can be used in Eqs. (7)-(10)-(11) to calculate the magnitudes of ψ_p and ϕ'_p. This is done for the physical model test using the measurements of stresses from the miniature pressure transducers and relative density calculated from the density cans. Accordingly, the values of ϕ'_p and ψ_p in the model test are 44.3^0 and 27^0, respectively. Alternative to Bolton (1986) equation, the magnitude of ψ_p can be predicted using the equation proposed by Cinicioglu and Abadkon (2015):

$$\phi'_p = \phi'_c + r\psi_p \tag{12}$$

Here in Eq. (12), α_ψ and m_ψ are unit-independent fitting parameters and I_D is relative density index. Unlike Bolton (1986) equation which is calibrated for the failure stress state, the equation proposed by Cinicioglu and Abadkon (2015) uses pre-shear mean effective stress (p'_i). The equation is unit-independent as p'_i is normalized with p_a which stands for standard atmospheric pressure at sea level.

Using the values of model backfill's D_{50} and ψ_p on the design chart given in Fig. 6, the magnitude of $\varepsilon_{q\text{-}f}$ is predicted as 0.651%. At this stage, the goal is to compare the predicted value with the $\varepsilon_{q\text{-}f}$ experimentally obtained from the model test.

The magnitude of $\varepsilon_{q\text{-}f}$ is obtained by PIV analyses of the model test photographs. The results of the PIV analyses for different stages of the model test are shown in Fig. 9. The successive images visually show the emergence and evolution of the shear band. As observed there, when the translation of the model wall approaches 1 mm, the shear band starts to emerge heralding the imminent failure of the backfill soil. When the amount of translation exceeds 1 mm, failure wedge becomes clearly visible indicating active failure.

Distributions of shear strains along the shear band's cross-section for different magnitudes of wall translation are shown in Fig. 10. On the other hand, Fig. 10 shows the increase in $\varepsilon_{q\text{-}f}$ with normalized wall displacement. The magnitude of $\varepsilon_{q\text{-}f}$ before active failure is within the range 0.65% to 1.3%. Because of the discrete state of photographs that are used in the PIV analyses, it is not possible to pinpoint the exact value of $\varepsilon_{q\text{-}f}$. However, it is noted that $\varepsilon_{q\text{-}f}$ predicted using Fig. 6 is within the experimentally obtained $\varepsilon_{q\text{-}f}$ range.

6. Proposed methods

Following the verification of the design chart, a step by step method is proposed for the selection of the design friction angle in practical applications:

i. ψ_p is determined either by calculation using Bolton (1986) or Cinicioglu and Abadkon (2015) equations or by testing.

ii. D_{50} value is obtained from sieve analysis.

iii. Using D_{50} and ψ_p values in the proposed design chart (Fig. 6), $\varepsilon_{q\text{-}f}$ is estimated.

iv. In order to estimate ε_q that would develop in the soil if the proposed structure is allowed to deform to its permissible limits ($\varepsilon_{q\text{-}max}$), proposed structure is modeled numerically. Displacements corresponding to the serviceability limits are imposed on the numerical model of the proposed structure via prescribed displacements and the resulting $\varepsilon_{q\text{-}max}$ is obtained.

v. If $\varepsilon_{q\text{-}f} > \varepsilon_{q\text{-}max}$, then ϕ'_p is used in design. However, if $\varepsilon_{q\text{-}f} \leq \varepsilon_{q\text{-}max}$, then ϕ'_c must be preferred.

Nevertheless the condition $\varepsilon_{q\text{-}f} \leq \varepsilon_{q\text{-}max}$ does not necessarily mean failure for the soil body. It is just an indication of the inception of a shear band because for most of the body of soil the magnitudes of ε_q are less than $\varepsilon_{q\text{-}f}$.

Using the empirical equations for prediction of ψ_p will require obtaining the necessary line-fitting parameters. However, the database on the necessary line-fitting parameters for different types of sands is steadily improving. The other parameter required for using Fig. 6 is D_{50}. Obtaining D_{50} is a straightforward task in practice and its value for the soils are routinely reported in site investigation reports. Once both ψ_p and D_{50} are obtained,

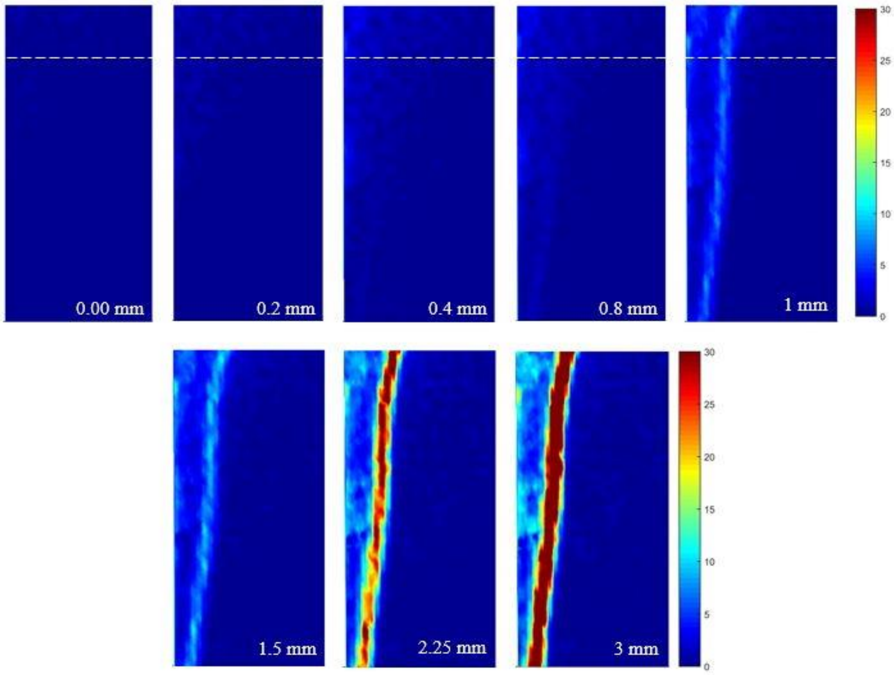

Fig. 9 Evolution of shear band at different stages of model wall translation

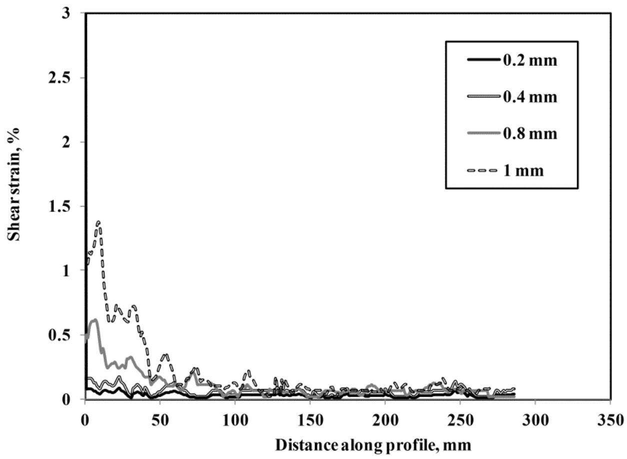

Fig. 10 Distribution of shear strain along the profiles selected in Fig. 9

the magnitude of ε_{q-f} can be determined using Fig. 6, which is then compared with the magnitude of the predicted ε_{q-max}. The magnitude of ε_{q-max} can be determined by modelling the proposed project and imposing the displacements corresponding to the serviceability limits on the modelled structure. This requires the use of any program based on either finite element method or finite difference method that allows the definition of correct geometry and boundary conditions for the problem under consideration. Constitutive models that more realistically simulate stress-strain response of the examined soils would be more accurate in predicting the possible magnitudes of ε_{q-max}. However, even simpler constitutive models such as Mohr-Coulomb would be useful depending on the precision of the laboratory and field tests from which the necessary model parameters are obtained. In any case, the precision of the predicted ε_{q-max} will mainly depend on the quality of the stiffness parameters, because at the serviceability limits the system will be away from failure. Since the serviceability limits of a structure depend on the permissible levels of displacements, the magnitudes and types of the displacements to be imposed on the structure in the numerical model requires the considerations and the input of the structural design engineer. With the use of this method, it becomes possible to select a design friction angle in geotechnical design in a structured way by taking into account both material properties and structural considerations.

7. Conclusions

For granular materials, there are two definitions of strength: peak strength and critical state strength. Accordingly, friction angle has two different values: peak and critical state friction angles. In geotechnical engineering, either of the two is selected as the design friction angle. However, this selection is an engineering choice which is generally based on the experience, intuition and preferences of the designer. This work attempts to propose an empirical method for guiding this selection. For this purpose, results of numerous triaxial tests are collected for ten different sands. Using the collected data, the relationship between magnitude of shear strain corresponding to failure and peak dilatancy angle is investigated. An empirical design chart based on peak dilatancy angle and mean grain diameter of the soil is developed. This design chart allows the estimation of the magnitude of shear strain corresponding to failure. A small-scale physical model test is conducted and the developed design chart is validated. Finally, a methodology is proposed for the selection of the design friction angle based on the serviceability limits of the proposed structure. With the proposed methodology, the predicted magnitude of shear strain corresponding the peak failure is compared with the predicted maximum shear strain the soil will experience at the serviceability limit of the system. Magnitude of maximum shear strain is obtained by imposing displacements that correspond to structural serviceability limits on the numerical model of the proposed structure. In cases where predicted magnitude of maximum shear strain is less than the predicted magnitude of shear strain at peak failure, peak friction angle can be used in design. Otherwise, critical state friction angle is used.

Acknowledgments

The authors would like to thank The Scientific and Research Council of Turkey (TUBITAK) for supporting this study with Project number 114M329.

References

Abadkon, A. (2012), "Strength and dilatancy of anisotropic cohesionless soils", Ph.D Dissertation, Bogazici University, Istanbul, Turkey.

Altunbas, A., Soltanbeigi, B. and Cinicioglu, O. (2017), "Determination of active failure surface geometry for cohesionless backfills", *Geomech. Eng.*, **12**(6), 983-1001. https://doi.org/10.12989/gae.2017.12.6.983.

Arda, C. (2019), "Influence of grain characteristics on stress-dilatancy relationship and failure surface geometry", Ph.D Dissertation, Bogazici University, Istanbul, Turkey.

Arda, C. and Cinicioglu, O. (2019), "Kohezyonsuz zeminlerin tane dagilim ve sekil ozelliklerinin aktif gocme yuzeyi geometrisine etkileri", *Teknik Dergi*, **30**(5), 9399-9420. https://doi.org/10.18400/tekderg.397658.

Bardet, J.P. (1997), *Experimental Soil Mechanics*, Prentice Hall, Upper Saddle River, New Jersey, U.S.A.

Bolton, M.D. (1986), "The strength and dilatancy of sands", *Géotechnique*, **36**(1), 65-78. https://doi.org/10.1680/geot.1986.36.1.65.

Bond, A. and Harris, A. (2008), *Decoding Eurocode 7*, CRC Press, London, U.K.

Chakraborty, T. and Salgado, R. (2010), "Dilatancy and shear strength of sand at low confining pressures", *J. Geotech. Geoenviron. Eng.*, **136**(3), 527-532. https://doi.org/10.1061/(ASCE)GT.1943-5606.0000237.

Cinicioglu, O. and Abadkon, A. (2015), "Dilatancy and friction angles based on in situ soil conditions", *J. Geotech. Geoenviron. Eng.*, **141**(4), 06014019. https://doi.org/10.1061/(ASCE)GT.1943-5606.0001272.

Cinicioglu, O. and Sancak, E. (2019), "Data for: Selection of design friction angle: A strain based empirical method for cohesionless soils", *Mendeley Data*, V1, https://doi.org/10.17632/rmwjbrgxxn.1.

de Bono, J.P. and McDowell, G.R. (2018), "Micro mechanics of drained and undrained shearing of compacted and overconsolidated crushable sand", *Géotechnique*, **68**(7), 575-589. https://doi.org/10.1680/jgeot.16.P.318.

Erzin, Y. (2004), "Strength of different anatolian sands in wedge shear, triaxial shear, and shear box tests", Ph.D Dissertation, Middle East Technical University, Ankara, Turkey.

Gezgin, A.T. and Cinicioglu, O. (2019), "Consideration of locked-in stresses during backfill preparation", *Geomech. Eng.*, **18**(3), 247-258. https://doi.org/10.12989/gae.2019.18.3.247.

Houlsby, G. (1991), "How the dilatancy of soils affects their behavior", *Proceedings of the 10th European Conference on Soil Mechanics and Foundation Engineering,* Florence, Italy, May.

Kazemi, M. and Bolouri, J.B. (2018), "A curtain traveling pluviator to reconstitute large scale sand specimens", *Geomech. Eng.*, **14**(2), 131-139. https://doi.org/10.12989/gae.2018.14.2.131.

Lee, K.L. and Seed, H.B. (1967), "Drained strength characteristics of sands", *J. Soil Mech. Found. Div.*, 117-139.

Muir Wood, D. (1990), *Soil Behaviour and Critical State Soil Mechanics*, Cambridge University Press, New York, U.S.A.

Ramos, C., Viana da Fonseca, A. and Vaunat, J. (2015), "Modeling flow instability of an Algerian sand with the dilatancy rule in CASM", *Geomech. Eng.*, **9**(6), 729-742. https://doi.org/10.12989/gae.2015.9.6.729.

Rowe, P.W. (1969), "The relation between the shear strength of sands in triaxial compression, plane strain and direct", *Géotechnique*, **19**(1), 75-86. https://doi.org/10.1680/geot.1969.19.1.75.

Rowe, P.W. (1962), "The stress-dilatancy relation for static equilibrium of an assembly of particles in contact", *Proc. Royal Soc. London Ser. A Math. Phys. Sci.*, **269**(1339), 500-527.

Samanta, M., Punetha, P. and Sharma, M. (2018), "Effect of roughness on interface shear behavior of sand with steel and concrete surface", *Geomech. Eng.*, **14**(4), 387-398. https://doi.org/10.12989/gae.2018.14.4.387.

Sancak, E. (2014), "Strain based selection of friction angle for geotechnical design", M.Sc Thesis, Bogazici University, Istanbul, Turkey.

Sasitharan, S. (1989), "Stress path dependency of dilatancy and stress-strain response of sand", Ph.D Dissertation, University of British Columbia, Vancouver, Canada.

Schanz, T. and Vermeer, P.A. (1996), "Angles of friction and dilatancy of sand", *Géotechnique*, **46**(1), 145-151. https://doi.org/10.1680/geot.1996.46.1.145

Skempton, A.W. and Bishop, A.W. (1950), "The measurement of the shear strength of soils", *Géotechnique*, **2**(2), 90-108. https://doi.org/10.1680/geot.1950.2.2.90.

Soltanbeigi, B., Altunbas, A. and Cinicioglu, O. (2019), "Influence of dilatancy on shear band characteristics of granular backfills", *Eur. J. Environ. Civil Engineering*, 1-18. https://doi.org/10.1080/19648189.2019.1572542

Stanier, S.A., Blaber, J., Take, W.A. and White, D.J. (2016), "Improved image-based deformation measurement for geotechnical applications", *Can. Geotech. J.*, **53**(5), 727-739. https://doi.org/10.1139/cgj-2015-0253.

Taylor, D.W. (1948), *Fundamentals of Soil Mechanics*, John Wiley & Sons, New York, U.S.A.

Tengattini, A., Das, A. and Einav, I. (2016), "A constitutive modelling framework predicting critical state in sand undergoing crushing and dilation", *Géotechnique*, **66**(9), 695-710. http://dx.doi.org/10.1680/jgeot.14.P.164.

White, D.J., Take, W.A. and Bolton, M.D. (2003), "Soil deformation measurement using particle image velocimetry (PIV) and photogrammetry", *Géotechnique*, **53**(7), 619-631. https://doi.org/10.1680/geot.53.7.619.37383.

CC